GEOCHEMISTRY

Ice-VII inclusions in diamonds: Evidence for aqueous fluid in Earth's deep mantle

O. Tschauner,[1]* S. Huang,[1] E. Greenberg,[2] V. B. Prakapenka,[2] C. Ma,[3] G. R. Rossman,[3] A. H. Shen,[4] D. Zhang,[2,5] M. Newville,[2] A. Lanzirotti,[2] K. Tait[6]

Water-rich regions in Earth's deeper mantle are suspected to play a key role in the global water budget and the mobility of heat-generating elements. We show that ice-VII occurs as inclusions in natural diamond and serves as an indicator for such water-rich regions. Ice-VII, the residue of aqueous fluid present during growth of diamond, crystallizes upon ascent of the host diamonds but remains at pressures as high as 24 gigapascals; it is now recognized as a mineral by the International Mineralogical Association. In particular, ice-VII in diamonds points toward fluid-rich locations in the upper transition zone and around the 660-kilometer boundary.

The water content of Earth's mantle is a key parameter of Earth's water budget (*1*). Global recycling of water in Earth drives important forms of volcanism such as island arcs (*2*, *3*), controls upper-mantle rheology (*4*), and plays a role in the evolution of mantle plumes (*5*). Subducted oceanic crust dehydrates at shallow depth (*2*, *3*), whereas faster and colder slabs can carry water much deeper (*6*). Average water abundance in the mantle changes markedly across the boundary between the upper mantle (UM) and the transition zone (TZ), as well as across the boundary between the TZ and the lower mantle (LM). These boundaries originate in the pressure-driven phase transformations of mantle rock minerals—in particular, the transformations of olivine to wadsleyite at 410 km and from ringwoodite to bridgmanite and periclase at 660 km depth. The UM contains only modest amounts of water on average (*7*), whereas the average water content in the TZ has been estimated at ~0.1 weight percent (*8*), or more than 10 times that of the UM. The abundance of water in the LM is unknown, but its constituent minerals appear to have much lower solubility of water than the minerals of the TZ (*9*, *10*). The average abundance of chemically bound water in these different regions of Earth, as well as possible occurrences of smaller layers or loci of water-rich rock or melt, are central to our understanding of Earth's water budget over extended geologic time. Furthermore, fluids and water-assisted partial melting mobilize mantle-incompatible elements, including heat-generating K, Th, and U. Previous models have proposed that upwelling mantle releases water while crossing the TZ-UM boundary and generates a buoyant layer of a comparatively water-rich melt that accounts for much of Earth's budget of heat-generating elements (*11*). Further, downward-moving material that crosses the TZ-LM boundary may lose its chemically bound water upon transformation into the LM minerals bridgmanite and periclase, thus triggering mantle metasomatism around the 660-km boundary (*10*, *11*).

The actual water content of different mantle regions depends not only on thermodynamic limits on water solubility but also on the mechanism in real Earth that carries water to beyond 410 km depth (*1*). The question of water abundance in the deeper mantle can therefore only be decided on the basis of actual samples from these regions whose mineralogical or petrographic record is placed in context with geochemical and geophysical observations, such as seismic wave attenuation and electrical conductivity (*1*, *4*, *8*), and by using experimentally obtained thermodynamic properties. Diamond is the main source of minerals from the deeper mantle: A mineralogical record from depths as great as 660 km or even beyond has been identified as inclusions in natural diamonds (*12*, *13*). Pearson *et al.* (*14*) reported an inclusion of hydrous ringwoodite in diamond from below 520 km depth whose formation implies a much more hydrous environment than the UM average. Generally, peridotitic diamonds mark regions of mantle metasomatism (*15*). Over long geologic time, metasomatism is almost pervasive, at least in Earth's UM. Diamonds conserve important information about these important processes (*16*).

Here, we provide evidence for the presence of aqueous fluid in regions of the TZ and around the TZ-LM boundary by showing the presence of ice-VII as inclusions in diamonds from these regions of the mantle. Ice-VII has recently been recognized as a mineral by the International Mineralogical Association [2017-029 (*17*)] (Table 1) on the basis of x-ray diffraction data that are presented here (Fig. 1). Ice-VII is a high-pressure form of water ice that is stable above 2.4 GPa (*18*). As we show, ice-VII (along with magnesian calcite, ilmenite, and halite) sensitively records high remnant pressures, which then also constrain the pressure and temperature where it has been encapsulated in the host diamond crystal, similar to other micrometer-scale inclusions of soft molecular materials such as CO_2, CO_2-H_2O, and N_2 in diamond (*19*–*23*).

By retaining high pressures, ice-VII inclusions monitor the former presence of H_2O-rich fluid at different depths in the diamond-bearing mantle. Remnants of former fluids and melts have been found as inclusions in many diamonds through infrared (IR) spectroscopy and microchemical analysis (*19*, *22*). On the basis of IR spectroscopy, a lower-pressure ice phase, VI, has been reported as an inclusion in diamond (*24*), but the fact that aqueous fluid has been trapped in the TZ or LM and crystallized as ice-VII was previously unknown.

Diamonds from southern Africa (Orapa, Namaqualand), China (Shandong), Zaire, and Sierra Leone were examined by diffraction with hard x-rays (0.3344 Å) and a beam focused to 2 μm × 3 μm at the undulator beamline 13-IDD (GSECARS, Advanced Photon Source, Argonne National Laboratory). A PILATUS 3X CdTe1M pixel array detector was used for collecting diffraction data. Diffraction from ice-VII was observed in diamonds from southern Africa and China as isolated arrays within the diamond matrix of dimensions ranging from 3 μm × 10 μm to less than 2 μm × 3 μm. Ice-VII was observed as isolated inclusions tens of micrometers afar from other inclusions, in proximity to small amounts of nickeliferous carbonaceous iron (Fig. 1), similar to metal inclusions reported in earlier studies on diamond (*24*), to ilmenite, and, in one case, to alkali halides. Many inclusions, such as silicates, carbonates, oxides, and halides, were observed through x-ray fluorescence mapping, some of which could be clearly identified through diffraction or microchemical analysis (Table 1). The observation of olivine with 94 to 97 mol % forsterite component (Fo 94-97) places the origin of the hosting diamonds in mantle peridotite rather than eclogite, whereas ilmenite is indicative of metasomatized mantle (*15*).

In all cases, the diffraction pattern of ice-VII is powderlike with no visible granularity (Fig. 1, inset). The patterns were unambiguously identified by Rietveld refinement as those of ice-VII (Table 1 and Fig. 1) (*26*) and correlate with IR absorption bands of O-H stretching vibrations (*26*). The high quality of some of the diffraction data resulted in noticeable proton contributions to the patterns (Fig. 1). Aqueous fluid in Earth's mantle is expected to be saline (*22*) and ice-VII can dissolve at least up to ~2 mole percent (mol %) of alkali halides (*27*, *28*). For structure analysis and for the assessment of pressure, dissolution of (Na,K)Cl has been taken into consideration. We provide details about the crystallography of natural ice-VII in (*26*); here, we focus on the

[1]Department of Geoscience, University of Nevada, Las Vegas, NV 89154, USA. [2]Center of Advanced Radiation Sources, University of Chicago, Chicago, IL 60637, USA. [3]Division of Geology and Planetary Science, California Institute of Technology, Pasadena, CA 91125, USA. [4]Gemological Institute, China University of Geosciences, Wuhan 430074, China. [5]School of Ocean and Earth Science and Technology, University of Hawai'i at Manoa, Honolulu, HI 96822, USA. [6]Royal Ontario Museum, Toronto, Ontario M5S 2C6, Canada.
*Corresponding author. Email: olivert@physics.unlv.edu

petrologic implications. We note that, with one exception (Table 1), the total salinity of the observed inclusions (ice-VII plus coexisting phases) is much lower than the alkali halide content of fluid inclusions commonly observed in diamonds. These inclusions also contain high amounts of silicate or carbonate (*22*). Many inclusions of silicates, carbonates, oxides, and halides are found within distances of several tens to 100 μm from the ice-VII inclusions. Plausibly, some of these phases that have been encapsulated at the same depth are precipitates from one complex fluid. We propose that a complex aqueous fluid was entrapped as separate inclusions that crystallized as ice-VII, carbonate, halide, and silicate rather than mimicking the bulk fluid composition in each inclusion (*26*).

Because of their confinement by the rigid diamond host crystal, the inclusions of ice-VII remain at high pressure, allowing us to use the equation of state of ice-VII to determine minimum pressures for formation of the surrounding diamond (Table 1). We found pressures of about 6 GPa and 9 ± 1.6 GPa for diamonds from Orapa, Botswana. We determined a pressure of 12 ± 2 GPa for a diamond from Shandong, China, and 24 to 25 (±3) GPa for a specimen from Namaqualand. In the fibrous rim of one diamond, we found a NaCl hydrate at a pressure of at least 1 GPa, rather than ice-VII (Table 1). We note that this sample was found at the same locality as three of the samples with inclusions around 6 and 9 GPa (Orapa, Botswana). Thus, ice-bearing diamonds from one location are not from the same source region or underwent additional growth at shallow depth. However, diamonds from geologically different locations such as China and southern Africa contain ice inclusions that reside at high pressures of 9 to 12 GPa (Table 1). Differences in nitrogen aggregation also indicate markedly different geologic ages or temperatures of the host diamonds and overall low nitrogen aggregation (*26*). Of 13 occurrences of ice-VII, eight fall into a narrow pressure

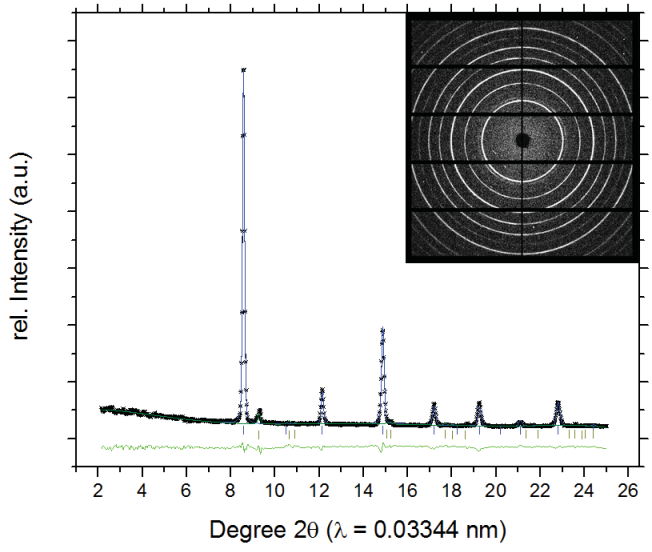

Fig. 1. Diffraction pattern of ice-VII in diamond M57666 from Orapa. Black crosses are data points; the Rietveld refinement based on this pattern of the type material (blue curve) converged to a weighted profile refinement parameter R_{wp} of 5.72% with a profile refinement parameter R_p of 4.57% and with $\chi^2 = 1.71$ for 1398 observations. The structure factor–based refinement parameter R_F was 4.0% (see table S3). The green line indicates the residual of fit. Blue tick marks denote symmetry-allowed reflections of ice-VII; olive tick marks denote allowed reflections of (Fe,Ni,C). (Fe,Ni,C) contributes 0.75 ± 0.05 volume percent to the pattern. The equation of state (*27*) allows estimation of the current pressure of this inclusion of ice-VII as 9.2 ± 1.6 GPa. The inset is a diffraction image of ice-VII. A diffraction image of ice-free diamond ~20 μm afar was used as a background image. Remaining single-crystal reflections are from the hosting diamond.

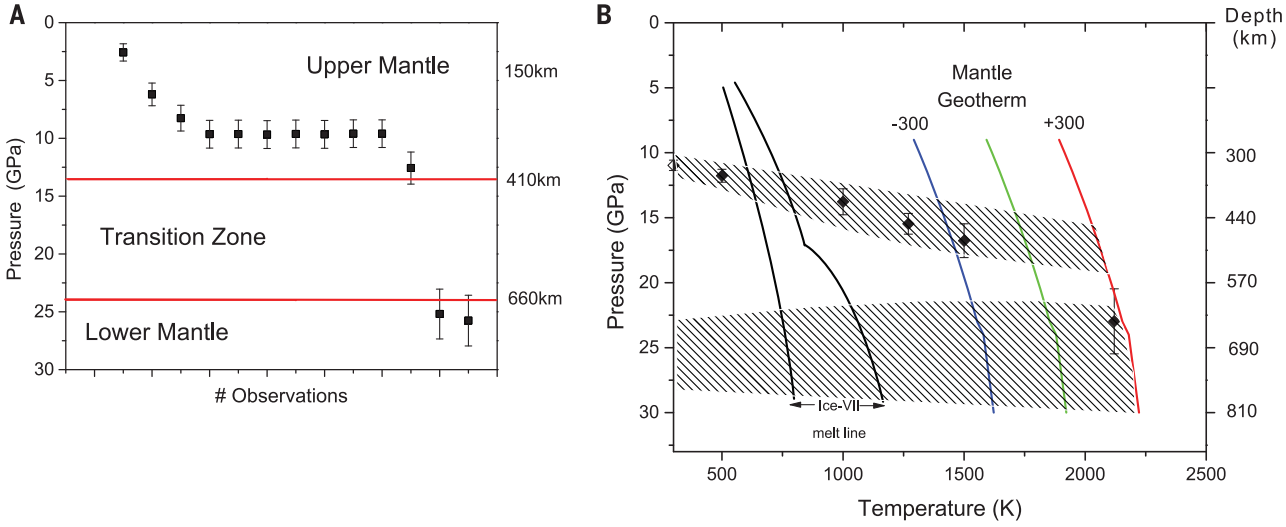

Fig. 2. Pressures of occurrences of ice-VII in natural diamonds. (**A**) Current residual pressures (black squares; error bars denote SD). These residual pressures also represent lower bounds of the pressures of entrapment. Thirteen inclusions have been identified with pressures ranging from >1 to 25 (±3) GPa. The majority of inclusions have residual pressures around 9 GPa. Red lines indicate the transitions between UM and TZ and between TZ and LM. (**B**) Reconstruction of entrapment conditions. We used the equations of state of diamond and fluid H_2O (*26*) to estimate plausible entrapment conditions. Current pressures were corrected for elastic relaxation of surrounding diamond (*33*). Within uncertainties, entrapment conditions can be estimated by the intersection of fluid H_2O isochores and mantle adiabats. We consider the current average mantle geotherm (*25*) and two adiabats that are 300 K hotter and cooler as a reference frame. The intersection of the isochores with these adiabats gives ranges of pressure of encapsulation of the aqueous fluid in growing diamond. We also show the entrapment path of ilmenite (black diamonds; error bars denote SD) with a residual pressure of 11 to 12 GPa that was found in ice-bearing diamond GRR1507 (Table 1). Simultaneous entrapment of ilmenite and fluid H_2O occurred at a pressure-temperature regime of 450 to 550 km depth and 1400 to 1900 K. The melting curve of ice-VII (*26*) is given for reference.

Table 1. Occurrences of ice-VII inclusions in diamond, number of occurrences, current pressure, and other observed inclusions. The assessment of pressure and its correction for elastic relaxation (P_{cor}) is described in (*26*). (Na,K)Cl·5H_2O has an ice-VII–like structure with Na + K + Cl residing on sites 2a and 4b (*26*). Volumes (μm^3) are approximate values based on integrated diffraction signal over the two-dimensional sampling grid; the depth was taken as an average of the two measured dimensions. A volume of 40 μm^3 corresponds to occurrences in single patterns. For weak single patterns, we assume a volume much smaller than 40 μm^3. Coexisting phases are defined as those observed in the same patterns as ice-VII; the phases may not be hosted by the same cavity. Errors in the last significant digit(s) are shown in parentheses.

Specimen	Ice-VII volume ($Å^3$)	(Na,K)Cl (mol %)	*P* (GPa)	P_{cor} (GPa)	O-H stretch and combination bands (cm^{-1})	Volume (μm^3)	Coexisting phases	Other phases
GRR1518	88.0(1)	16.8	≥1	—	3220(20)	<40	(Na,K)Cl, (Na,K)Cl·5H_2O	
GRR1507	33.689(8)	3(1)	6(1)	7(2)	3210(20)	<<40	Ilmenite† 85%	Olivine (Fo94-97),‡ calcite, sellaite
GRR1507	32.40(1)	<5	7.9(1.4)	9(2)	—	<40	Ilmenite† 81%	
GRR1521	31.647(5)	<0.1	9.2(1.6)	11(2)	3000 to 3100	<40	—	Garnet, olivine
M57666*	31.653(4)	4.4(6)	9.2(1.6)	11(2)	2950 to 3100	3000	(Fe,Ni,C) 0.75%	
GRR1521	31.632(5)	2.4(6)	9.3(1.6)	11(2)	—	500	(Fe,Ni,C) 59.7%	
GRR1521	31.658(8)	1.8(1)	9.2(1.6)	11(2)	—	500	(Fe,Ni,C) 0.7%	
GRR1521	31.641(5)	<0.1	9.3(1.6)	11(2)	—	<40	(Fe,Ni,C) 1.0%	
GRR1521	31.671(5)	3.6(4)	9.2(1.6)	11(2)	—	<40	(Fe,Ni,C) 1.3%	
GRR1521	31.6705(9)	<0.1	9.2(1.6)	11(2)	—	3000	—	
Balas-1	26.38(4)	3(1)	24(3)	28(5)	3140(20), 4500(50)	<40	—	Calcite, halite, sellaite,‡ chromite
Balas-3	26.25(9)	3(2)	25(3)	28(5)	—	<<40	—	
SM548	30.284(9)	2 to 5	12.0(2.0)	14(2)	3100(50)	<40	—	Calcite,§ halite,§ olivine

*Ice-VII type specimen. †(Ilm92-97 Geik3-8), $a = b = 5.0161(6)$ Å, $c = 13.686(4)$ Å. ‡Sellaite, MgF_2, olivine composition was measured by SEM-EDS from four different locations. §$(Ca_{0.75(2)}Mg_{0.25(2)})CO_3$, $a = b = 4.803(2)$, $c = 15.98(1)$ Å, which corresponds to 8 to 9 GPa (*26*); halite, $a = 5.231$ Å, which corresponds to 10(1) GPa (*26*).

interval around 8 to 12 GPa (Fig. 2A and Table 1). This pronounced clustering of sustained pressures and the observation of ice inclusions at 24 to 25 GPa have geologic implications: They point toward regions in the deep mantle where aqueous fluid was present during growth of diamond. We note that the sustained pressures of ice-VII inclusions match those of inclusions of ilmenite, magnesian calcite, and halite in the same host diamonds (Table 1) (*26*), indicating growth at similar depth.

We can attempt to go a step further and estimate the pressure under which the inclusions were trapped by correcting for the thermal contribution to pressure and volume caused by the high temperatures in the deeper mantle. This requires reconstruction of plausible paths that connect the current residual pressure of these inclusions with the pressures and temperatures of their possible host regions in the deep Earth. That temperature can be along the current average mantle geotherm, a possibly higher geothermal temperature in the geologic past, or a cooler regime in the vicinity of subducted slabs or within harzburgitic restites. Therefore, we encompass these different possible temperature-depth regimes by a reference frame defined through three adiabats whose temperatures include possible cool and hot regimes (*25*, *29*–*32*): the modern average mantle geotherm (*25*) plus two adiabats 300 K below and above this geotherm. This does not imply that the ice-bearing diamonds formed in a convecting mantle; rather, it defines a temperature-pressure range that includes different plausible source regions. We argue that within given uncertainties of thermoelastic properties, the pressure range of entrapment is constrained by the intersection of these adiabats, with pressure-temperature paths of the inclusions approximated as isochores (*19*, *20*) (Fig. 2B); see (*26*) for details. We note that our estimation of entrapment conditions for ice-VII and ilmenite overlap in the depth of the shallower TZ (Fig. 2B).

Two main conclusions can be drawn: (i) The aqueous inclusions were entrapped as fluid rather than solid ice (*32*). Crystallization into ice-VII has occurred at much shallower depth during ascent. (ii) Despite marked uncertainties in the equations of state, the entrapment pressures for the ice inclusions that are currently at ~8 to 12 GPa turn out to be sufficiently narrow to permit a statement of the depth of their source regions (Fig. 2B): They range from 400 to 550 km depth. For the inclusions at 24 to 25 GPa, the source region is less narrowly estimated at 610 to 800 km depth; 620 km is the depth of entrapment estimated for dense N_2 inclusions in diamond (*20*). Overall, the ice-VII inclusions show directly that water-rich fluid occurs in regions within the TZ and around the 660-km boundary, or possibly in the shallow LM (Fig. 2B). Taken together with the occurrence of magnesian calcite and halite at similar pressures, we can infer the presence of complex aqueous, saline, and carbonaceous fluid at those depths. At present, we cannot assess the extent of these fluid-rich regions, although it is plausible that they were constrained both in space and time before evolving into less hydrous partial melts.

The much lower compatibility of H_2O in the LM relative to the TZ (*9*, *10*) has been suggested to cause mantle metasomatism when slabs or surrounding mantle are sinking to below the 660-km boundary: H_2O that cannot be chemically bound by the bridgmanite-periclase phase assembly of the lower mantle is released and interacts with surrounding mantle (*10*, *11*). Our observation of ice and its plausible origin from a free aqueous fluid below 610 km depth (Fig. 2B) is consistent with this hypothesis and connects the experimental and geodynamic work with observations from nature. More generally, natural ice-VII, magnesian calcite, and halite provide new indicators for the presence of water-bearing and carbonaceous fluid in actual deep Earth samples, which can be linked to geochemical and geophysical information obtained from the same regions in Earth. Ice-VII and other micro-inclusions (Table 1) provide, through their residual density, an accurate minimal pressure of formation, although the reconstruction of the entrapment pressure at mantle temperatures is currently limited by the available thermoelastic data on aqueous (saline) fluid.

REFERENCES AND NOTES

1. S. Karato, in *Treatise on Geophysics*, G. Schubert, Ed. (Elsevier, 2015), pp. 105–144.
2. T. L. Grove, C. B. Till, E. Lev, N. Chatterjee, E. Médard, *Nature* **459**, 694–697 (2009).
3. S. G. Nielsen, H. R. Marschall, *Sci. Adv.* **3**, e1602402 (2017).
4. H. Jung, S. Karato, *Science* **293**, 1460–1463 (2001).
5. N. Métrich *et al.*, *J. Petrol.* **55**, 377–393 (2014).
6. L. H. Rupke, J. P. Morgan, M. Hort, J. A. D. Connolly, *Earth Planet. Sci. Lett.* **223**, 17–34 (2004).
7. D. R. Bell, G. R. Rossman, *Science* **255**, 1391–1397 (1992).

8. S. Karato, *Earth Planet. Sci. Lett.* **301**, 413–423 (2011).
9. T. Inoue, T. Wada, R. Sasaki, H. Yurimoto, *Phys. Eartheart Planet. Inter.* **183**, 245–251 (2010).
10. B. Schmandt, S. D. Jacobsen, T. W. Becker, Z. Liu, K. G. Dueker, *Science* **344**, 1265–1268 (2014).
11. D. Bercovici, S. Karato, *Nature* **425**, 39–44 (2003).
12. F. E. Brenker, T. Stachel, J. W. Harris, *Earth Planet. Sci. Lett.* **198**, 1–9 (2002).
13. T. Stachel, J. W. Harris, G. P. Brey, W. Joswig, *Contrib. Mineral. Petrol.* **140**, 16–27 (2000).
14. D. G. Pearson *et al*., *Nature* **507**, 221–224 (2014).
15. N. V. Sobolev *et al*., *Lithos* **39**, 135–157 (1997).
16. S. B. Shirey *et al*., *Rev. Mineral. Geochem.* **75**, 355–421 (2013).
17. O. Tschauner, E. Greenberg, V. Prakapenka, C. Ma, K. Tait, *Mineral. Mag.* **81**, 1033–1038 (2017).
18. V. F. Petrenko, R. W. Whitworth, *Physics of Ice* (Oxford Univ. Press, 1999), p. 253.
19. O. Navon, *Nature* **353**, 746–748 (1991).
20. O. Navon *et al*., *Earth Planet. Sci. Lett.* **464**, 237–247 (2017).
21. E. S. Izraeli, J. W. Harris, O. Navon, *Earth Planet. Sci. Lett.* **187**, 323–332 (2001).
22. Y. Weiss, I. Kiflawi, O. Navon, in *Proceedings of 10th International Kimberlite Conference* (Springer, 2013), pp. 271–280.
23. H. Kagi *et al*., *Mineral. Mag.* **64**, 1089–1097 (2000).
24. E. M. Smith *et al*., *Science* **354**, 1403–1405 (2016).
25. J. M. Brown, T. J. Shankland, *Geophys. J. R. Astron. Soc.* **66**, 579–596 (1981).
26. See supplementary materials.
27. M. R. Frank, E. Aarestad, H. P. Scott, V. B. Prakapenka, *Phys. Earth Planet. Inter.* **215**, 12–20 (2013).
28. L. E. Bové *et al*., *Proc. Natl. Acad. Sci. U.S.A.* **112**, 8216–8220 (2015).
29. C. Herzberg, K. Condie, J. Korenaga, *Earth Planet. Sci. Lett.* **292**, 79–88 (2010).
30. C. T. A. Lee, P. Luffi, T. Plank, H. Dalton, W. P. Leeman, *Earth Planet. Sci. Lett.* **279**, 20–33 (2009).
31. C. A. Dalton, C. H. Langmuir, A. Gale, *Science* **344**, 80–83 (2014).
32. C. R. Bina, A. Navrotsky, *Nature* **408**, 844–847 (2000).
33. R. J. Angel, M. L. Mazzucchelli, M. Alvaro, P. Nimis, F. Nestola, *Am. Mineral.* **99**, 2146–2149 (2014).

ACKNOWLEDGMENTS

We thank four anonymous reviewers for their helpful comments, and H. A. Bechtel for support at the Advanced Light Source. **Funding:** This work was supported by U.S. Department of Energy (DOE) awards DESC0005278, DE-FG02-94ER14466, and DE-NA0001974, and by NSF grants EAR-1634415, EAR-1128799, EAR-1322082, EAR-0318518, and DMR-0080065. The Advanced Photon Source, a DOE Office of Science User Facility, is operated by Argonne National Laboratory under contract DE-AC02-06CH11357. The Advanced Light Source is supported through contract DE-AC02-05CH11231. **Author contributions:** O.T. participated in design, interpretation, data collection, and analysis of the reported results, and in drafting and revising the manuscript; S.H. participated in interpretation of the results and in drafting and revising the manuscript; E.G., V.B.P., C.M., G.R.R., A.H.S., D.Z., and K.T. participated in data collection and revising the manuscript; and M.N. and A.L. participated in data collection. **Competing interests:** The authors have no competing interests. **Availability of data and materials:** Additional chemical and crystallographic information about ice-VII is provided as supplementary material. Raw data are deposited at Dryad (doi:10.5061/dryad.7145v). Crystallographic and chemical information on type material ice-VII are deposited with the ICSD database.

SUPPLEMENTARY MATERIALS

www.sciencemag.org/content/359/6380/1136/suppl/DC1
Materials and Methods
Figs. S1 to S4
Tables S1 to S3
References (*34*–*59*)

5 July 2017; accepted 19 January 2018
10.1126/science.aao3030

Ice-VII inclusions in diamonds: Evidence for aqueous fluid in Earth's deep mantle

O. Tschauner, S. Huang, E. Greenberg, V. B. Prakapenka, C. Ma, G. R. Rossman, A. H. Shen, D. Zhang, M. Newville, A. Lanzirotti and K. Tait

Science **359** (6380), 1136-1139.
DOI: 10.1126/science.aao3030

Encapsulating Earth's deep water filter

Small inclusions in diamonds brought up from the mantle provide valuable clues to the mineralogy and chemistry of parts of Earth that we cannot otherwise sample. Tschauner *et al.* found inclusions of the high-pressure form of water called ice-VII in diamonds sourced from between 410 and 660 km depth, the part of the mantle known as the transition zone. The transition zone is a region where the stable minerals have high water storage capacity. The inclusions suggest that local aqueous pockets form at the transition zone boundary owing to the release of chemically bound water as rock cycles in and out of this region.

Science, this issue p. 1136